Direct demonstration of photoluminescence originated from surface functional groups in carbon nanodots

CrossMark

Vanthan Nguyen [a, b], Jinhai Si [a, *], Lihe Yan [a], Xun Hou [a]

[a] Key Laboratory for Physical Electronics and Devices of the Ministry of Education and Shaanxi Key Lab of Information Photonic Technique, School of Electronics and Information Engineering, Xi'an Jiaotong University, Xi'an 710049, China
[b] Le Quy Don Technical University, Hanoi 122314, Vietnam

ARTICLE INFO

ABSTRACT

Carbon nanodots (C-dots) are promising substitutes for the present fluorescent nanomaterials of various applications due to their unique combination properties of intense photoluminescence (PL), low toxicity, and high aqueous solubility. However, the origin of the fascinating PL in C-dots is still a matter of current debate. Due to their complex and uncontrollable structures, the contributions of surface chemicals and carbogenic-core to their PL are poorly understood. Here, a facile two-step method combining laser ablation and UV light irradiation has been developed, in which non-fluorescent C-dots are prepared by ablating graphite powders in water using nanosecond laser, and the PL intensities are enhanced by UV light irradiation in oxygen atmosphere. Using this strategy, we are able to control the size and the surface functional groups of C-dots independently. By detailed characterization and comparison of different C-dots, we find that the intense PL in C-dots is originated from abundant surface functional groups on its surface rather than its carbogenic-core. One kind of surface functional group forms a single surface state energy level and becomes an isolated emission center with specific carrier dynamics on the surface site of C-dots. The energy gap of each surface state exhibits carbogenic-core size independent and is characterized by distinct central energies, such as C=O group at 335 nm, and C–O group at 430 nm.

© 2016 Elsevier Ltd. All rights reserved.

1. Introduction

Carbon nanodots (C-dots) have attracted rapidly growing interest in recent years due to their unique combination properties of intense photoluminescence (PL), high photostability, high aqueous solubility, low toxicity, and excellent biocompatibility [1,2]. Typically, C-dots have an sp^2 or amorphous carbon core with size less than 10 nm, and a surface coated with oxygen-, nitrogen-, or sulfur-containing functional groups that imparting them with excellent water solubility. To date, C-dots with intense PL can be readily produced on a large scale by many approaches include laser ablation [3,4], hydrothermal [5–7], ultrasound [8], and microwave-assisted synthesis [9]. As a result, C-dots are promising substitutes for the present fluorescent nanomaterials of various applications, such as biological imaging [5,6], drug delivery [10], sensors [11,12], light-emitting devices [13–15], and lasers [16,17]. Nonetheless, the origin of PL in C-dots is not clear to date, limiting

the effective synthesis of C-dots material with desired brightness and working wavelength for practical applications.

There have been several studies on the nature of the intense PL in C-dots. Some studies demonstrated the PL in C-dots was attributed to the emissions from both carbogenic-cores and surface functional groups, in which surface chemical modifications and changes in size also lead to changes in emission wavelength [18–21]. Nonetheless, recent reports have argued that the PL originates from surface functional groups only [22–24]. In accordance with the former proposed mechanism, several reports ascribed the PL red shift of C-dots to quantum confinement of carbogenic-core [25,26]. However, the origin of this emission has been a matter of debate due to: (i) diversity of C-dots prepared by various approaches; (ii) uncertainty and complexity of chemical groups on the surface induced during synthesis process [24,25]; (iii) difficulties to assess the influences of size and surface chemicals on the optical properties due to lack of means for independent control of size and surface chemical [26,27]; (iv) the emission spectra of C-dots are broad and lack of special properties for comparison [19,28,29].

In this work, we try to shed light on the origin of the intense PL

* Corresponding author.
  E-mail address: jinhaisi@mail.xjtu.edu.cn (J. Si).

in C-dots and its relation to their structural properties. C-dots adopted here are synthesized using a facile two-step approach combining nanosecond laser ablation and UV light irradiation. Using this strategy, we are able to control the size and the surface functional groups of C-dots independently. By comparing the structures and optical properties of these C-dots, we reveal that the PL of C-dots originates from abundant surface functional groups on its surface rather than its carbogenic-core, where each kind of surface functional group may become an isolated and characteristic emission center with size-independent energy gap.

2. Experimental

C-dots were synthesized via nanosecond laser ablation of graphite powders in distilled water. Typically, 20 mg of carbon powders, with a mean size of 400 nm, was dispersed into 50 ml distilled water via ultrasonication. Next, the suspension was put into a glass beaker for laser irradiation. The laser beam (Q-switched Nd: YAG laser, central wavelength: 1064 nm, pulse duration: 10 ns, and repetition rate: 10 Hz) was focused into suspension by 100 mm lens for 2 h. The average pulse energy was ranging from 0.5 to 15 mJ/pulse for fabrication of different size C-dots. During the laser irradiation, a magnetic stirrer was used to prevent gravitational settling of the suspended powders. Centrifugation was used to separate larger carbon nanoparticles and the pristine C-dots were obtained from the supernatant. After that, the pristine C-dots solution was bubbled with O_2 and irradiated by a hand UV lamp (365 nm) for different times.

Transmission electron microscopy (TEM) and high-resolution TEM (HRTEM) images of the C-dots were obtained via a high resolution transmission electron microscopy (model JEM-ARM200F). Through image analysis, the average diameter and size distribution was determined for ~1000 C-dots. A U-3010 spectrophotometer (Hitachi) was employed to measure the absorption spectra of the samples. The Fourier transform infrared (FTIR) spectroscopy was performed on a VERTEX 70 (Bruker) using KBr pellet method. X-ray photoelectron spectroscopy (XPS) experiments were carried out on AXIS ULtrabld (Kratos) X-ray photoelectron spectrometer. The PL characterizations including emission spectra, excitation spectra, fluorescence lifetimes, and time-resolved PL spectra were recorded using FLS920 spectrometer (Edinburgh). For the fluorescence lifetimes and time-resolved PL measurements, picosecond pulsed LEDs (central wavelength: 273, 343 nm, pulse duration: <850 ps, repetition rate: 10 MHz) were used as excitation sources.

3. Results and discussion

To independent control of the carbogenic-core size and surface functional groups, C-dots were synthesized by a two-step process, as shown in Fig. 1. First, pristine non-fluorescent C-dots were synthesized via nanosecond laser ablation of graphite powders in distilled water with different laser-pulse energies. When nanosecond pulses inject into the suspension, C-dots with size of several nanometers can be produced through laser-induced melting and evaporation of graphite powders [30]. The C-dots sizes can be well controlled by adjusting laser-pulse energy. In general, the mean size of C-dots progressively decreased with increases in laser-pulse energy [31]. Second, the C-dots were photo-oxidized by UV light irradiation of C-dots solution with bubble of O_2. Under UV light irradiation, O_2 can absorb photons to generate strongly oxidizing singlet oxygen and ozone, while photoexcited C-dots are highly active as electron donors. As a result, the surfaces of C-dots are oxidized [32]. The oxidation degree of C-dots might be controlled by adjusting irradiation time while the carbogenic-core size basically remains unchanged.
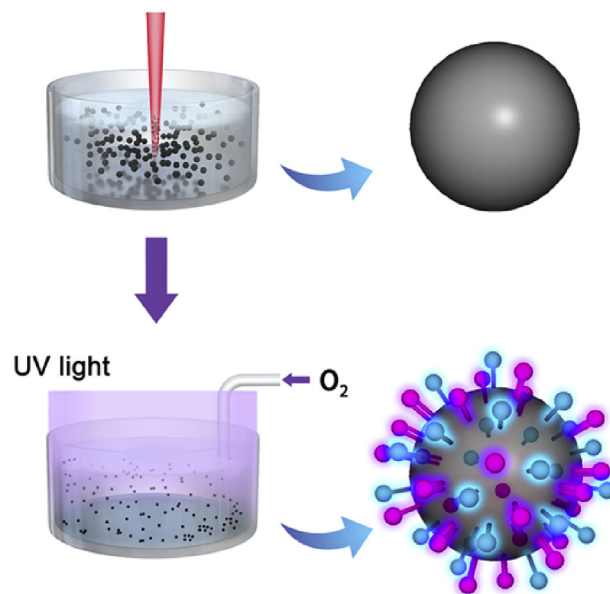

Fig. 1. Schematic illustration of the synthesis process of C-dots. First, pristine C-dots were synthesized via nanosecond laser ablation of graphite powders in distilled water with different laser-pulse energies. Second, the C-dots were photo-oxidized by UV light (365 nm) irradiation with bubble of O_2 for different times. (A colour version of this figure can be viewed online.)

Fig. 2a shows the TEM image of the pristine C-dots synthesized by laser ablation of graphite powders in distilled water at average pulse energy of 5 mJ/pulse. The pristine C-dots have small size distribution in the range of 1—2.5 nm with a mean diameter of 1.7 nm (Fig. 2b). HRTEM images of the pristine C-dots (Fig. 2c and d) show well-resolved crystal lattice fringes with a spacing of 0.21 nm which is very close to the (100) facet of graphite carbon [27]. Although the carbogenic-core structures of pristine C-dots are similar with C-dots prepared by other methods [33—35], there are basically no detectable fluorescence from the pristine C-dots. The PL spectra of distilled water dispersed with pristine C-dots present only Raman scattering of water (Supporting Information, Fig. S1). This indicates that laser ablation of graphite powders in water can fabricates pristine C-dots with well carbogenic-core structures and no PL emission.

To study the effect of surface chemicals on the PL properties of C-dots, the pristine C-dots were further photo-oxidized by UV light irradiation. The PL intensities of the C-dots are significantly enhanced and the maximum photoluminescence quantum yield (PLQY) can reach 2.1% (360 nm excitation) after several hours UV light irradiation (fluorescence images as Fig. S2). Although the PLQY is still low, the enhancement of PL intensity provides an important evidence for study of their PL mechanism. Fig. 3a—c shows the PL spectra of C-dots after 1, 2, and 4 h irradiation, respectively. Unlike many other reported C-dots exhibiting full-color or single fluorescence-peak emissions [24,26], all PL emissions of our samples exhibit two obviously fluorescence peaks, centered at 335 and 430 nm, and the fluorescence peaks do not shift when different excitation wavelengths were applied. The fluorescence peaks at 335 and 430 nm are alternately dominant when excitation wavelength changes. The energy shifts of optimal excitation wavelength and corresponding fluorescence peak are 0.73 and 0.56 eV for the peaks at 335 and 430 nm, respectively. These phenomena suggest the fluorescence peaks are originated from two independent emission centers in the C-dots. Two fluorescence peak intensities increase dramatically with irradiation time and reach maximum after 2 h
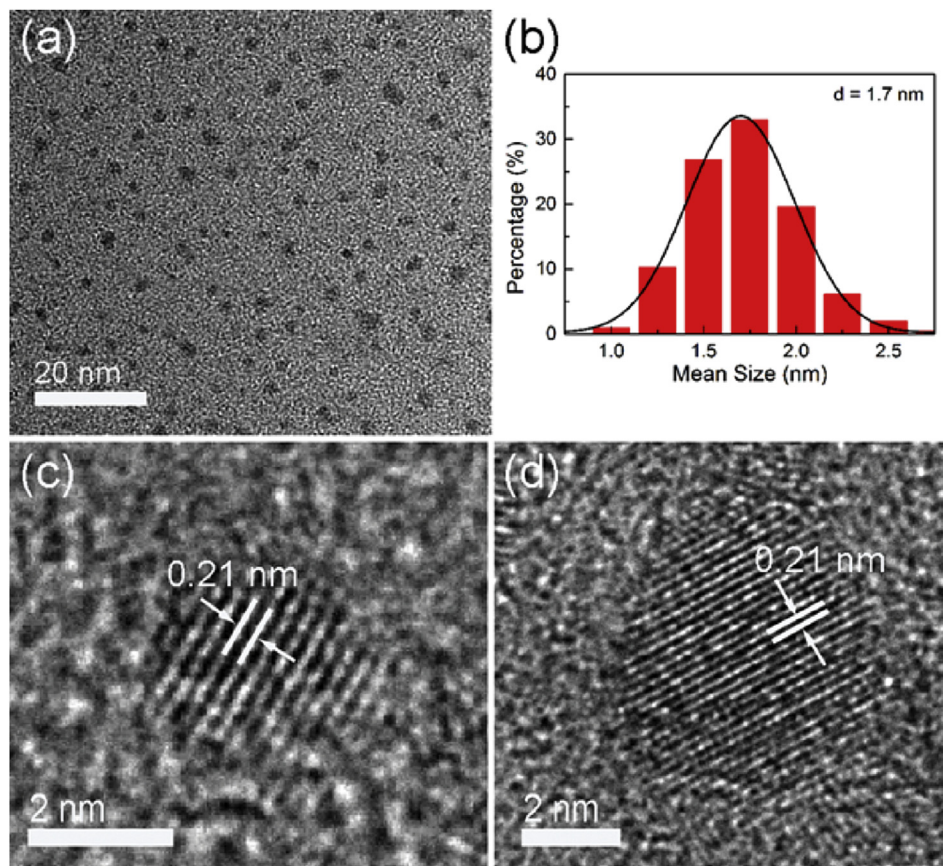
Fig. 2. (a) TEM image, (b) size distribution, and (c, d) HRTEM images of pristine C-dots synthesized by laser ablation of graphite powders in distilled water at average pulse energy of 5 mJ/pulse. (A colour version of this figure can be viewed online.)
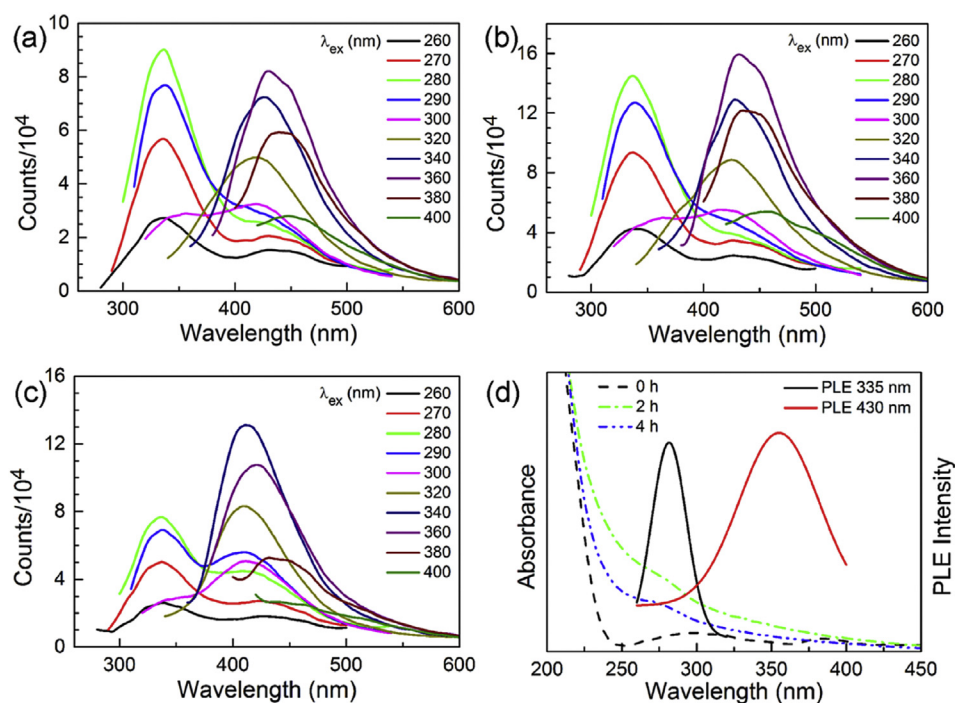

Fig. 3. (a, b, c) The PL spectra of the C-dots after 1, 2, and 4 h irradiation of UV light, respectively. (d) UV-vis absorption spectra of pristine C-dots, C-dots after 2 h, and C-dots after 4 h UV light irradiation (dotted lines); photoluminescence excitation (PLE) spectra of the C-dots after 2 h UV light irradiation detected at 335 and 430 nm (solid lines). (A colour version of this figure can be viewed online.)

irradiation. Further irradiation, however, decreased fluorescence and the intensity declines to half its maximum value after 7 h irradiation (Fig. S3). The dependence of fluorescence intensity of the C-dots on irradiation time might be attributed to massive oxidation of the surface of C-dots [32].

The PL enhancement of C-dots after photo-oxidation might be attributed to the emission from new-created functional groups on the surface. First, TEM and HRTEM images of C-dots after UV light irradiation (Fig. S4) show no evident difference compared with that of initial pristine C-dots. The mean sizes of C-dots basically remain unchanged after UV light irradiation, i.e. 1.7 nm. Thus, the effect of carbogenic-core structure on PL enhancement can be excluded. Second, there are two new bands in UV-vis absorption spectra of the C-dots after UV light irradiation (Fig. 3d), indicating new surface groups have been created [24,27]. One is located at around 280 nm, which is attributed to n-π^* transition of C=O bonds [20]. The other is subtle and centered about 355 nm with a tail, which is assigned according to previously reports [33,36]. Due to the overlapping with the absorption of carbon backbones, the absorption bands seem weak and subtle. However, these absorption bands could be identified by subtracting the background absorption of pristine C-dots (Fig. S5). These absorption bands are also evident in photoluminescence excitation (PLE) spectra (Fig. 3d). The PLE spectra of the fluorescence peaks at 335 and 430 nm exhibit strong exciting bands centered around 280 and 355 nm, respectively. The results suggest that the fluorescence peaks at 335 and 430 nm are originated from two new-created functional groups on the surface of C-dots.

The chemical compositions and structures of these C-dots are further investigated using FTIR and XPS analysis. The FTIR spectra shown in Fig. 4a reveal that all C-dots show similar intensity of stretching vibration of O—H bond at 3420 cm^{-1}. However, compared with pristine C-dots, new vibration bands of C=O double bond at 1630 cm^{-1} and C—O bond at 1045 cm^{-1} were observed in the C-dots after UV light irradiation. The results reveal that two new functional groups are created on C-dots after UV light irradiation while the original surface group, i.e. O—H bond, remains unchanged.

More information about the differences in surface functional groups of C-dots before and after UV light irradiation is further provided by XPS analysis. The XPS survey spectra (Fig. S6) show that only carbon (C 1s, 285 eV) and oxygen (O 1s, 533 eV) elements were contained in these C-dots and the intensity of O 1s peak gradually increases with increasing irradiation time. The high-resolution C 1s spectrum of pristine C-dots (Fig. 4b) shows two peaks: a strong peak at 284.6 eV corresponds to C=C bond, and the other is subtle at 286.0 eV ascribed to C—O bond [35]. The content of C=C bond is 96.4% and that of C—O bond is 3.6%. This indicates that the pristine C-dots possess graphitic carbogenic-core with very few surface functional groups on the surface. As comparisons, the C 1s spectra of C-dots after 2 and 4 h UV light irradiation can be deconvoluted into three surface contents, that is, C=C at 284.5 eV, C—O at 286.0 eV, and C=O at 287.9 eV (Fig. 4c and d). The contents of both C—O and C=O groups significant increase with irradiation time (Table S1) and the content of C—O group can reaches ~60% after 4 h irradiation. The results indicate C—O and C=O groups with large quantity are created after UV light irradiation. The fact that only two types of functional groups form after UV light irradiation is also supported by the appearance of only C—O and C=O groups in their high-resolution O 1s spectra (Fig. S7). Furthermore, the content ratio between C—O and C=O groups in C-dots after 2 h irradiation is 3.1 and increases to 4.8 for C-dots after 4 h irradiation, which is consistent with the increase of their fluorescence peak intensity ratio at 430 and 335 nm. Thus, we suggest that the strong fluorescence peaks at 335 and 430 nm in C-dots after UV light irradiation are originated from C=O and C—O groups, respectively.

Results enumerated above prove that the intense fluorescence in C-dots is originated from abundant surface functional groups on its surface, rather than originating from its carbogenic-core. One kind of surface functional group forms a surface state energy level
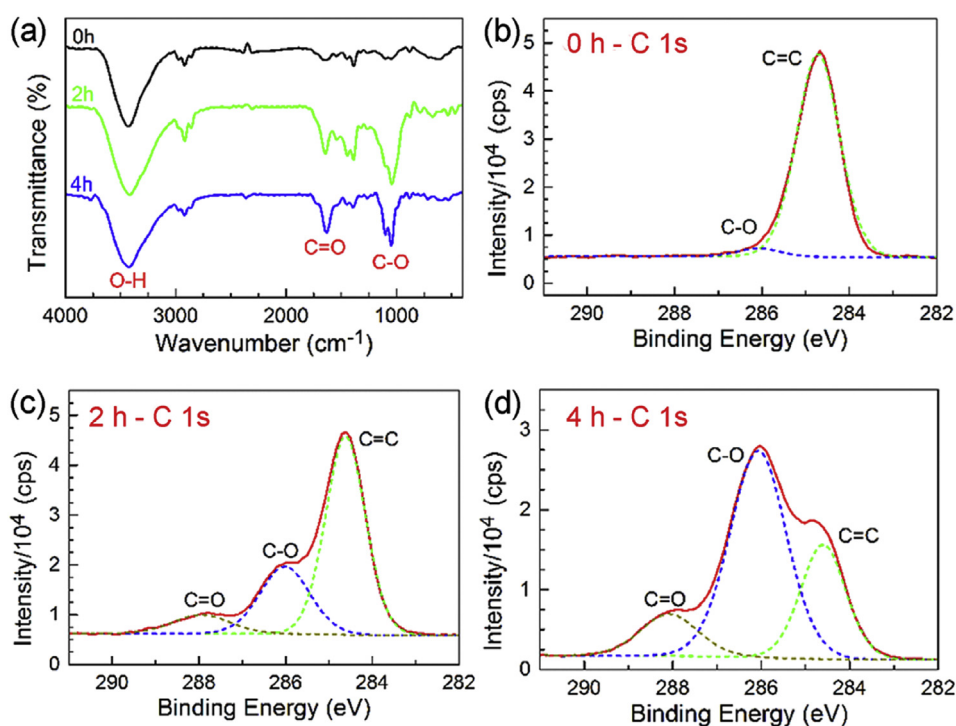

Fig. 4. (a) FTIR spectra of pristine C-dots, C-dots after 2 h, and C-dots after 4 h UV light irradiation. (b, c, d) High-resolution C 1s XPS spectra of pristine C-dots, C-dots after 2 h, and C-dots after 4 h UV light irradiation, respectively. (A colour version of this figure can be viewed online.)

and becomes an isolated emission center [22]. Each of the surface states is likely distributed in energy; however, these distributions are characterized by distinct central energies, such as C=O group at 335 nm, and C–O group at 430 nm. This conclusion is supported by the similar fluorescence peak position of C-dots at different reports, in which different synthesis methods were applied [27,37]. Because of their distinct energy distribution, each of the surface states can be excited with a specific range of wavelengths such as 260–300 nm for C=O group, and 300–380 nm for C–O group. The surface states are in turn excited and the dominant emission alternates when the excitation wavelength changes. Subsequently, C-dots with abundant surface functional groups might exhibit excitation-dependence and full-color emission [27]. Furthermore, C-dots with larger quantity of surface functional groups and less surface defects, a stronger PL can be expected. As the C-dots presented here, the fluorescence peak intensities basically increase with contents of C–O and C=O groups. For C-dots with longer irradiation times (>2 h), the increase of oxidation degree accompany with increasing surface defects (nonradiative states) due to photocorrosion [32], subsequently decreasing PL intensity [22].

To study the effect of carbogenic-core size to the PL properties of C-dots, experiments of pristine C-dots with different sizes were carried out. The pristine C-dots with mean sizes of 1.1, 3.6, and 5.5 nm were also synthesized by using different laser powers (TEM images shown in Fig. S8). All of these C-dots are similar with the pristine C-dots discussed above that exhibit no detectable PL. After 2 h UV light irradiation, the strong fluorescence peaks centered at 335 and 430 nm are also observed. The fluorescence peak positions at 335 and 430 nm basically remain unchanged with variation of C-dots size (Fig. S9). The results indicate that the emission centers from surface functional groups in C-dots are size independent.

To explore the carrier dynamics in C-dots, the time-resolved PL spectra and fluorescence lifetime of the C-dots after 2 h UV light irradiation were monitored. The time-resolved PL spectra of the C-dots at 273 nm excitation are shown in Fig. 5a. The PL maximum does shift on time scales from 0.1 to 4 ns, which is similar with the maximum of steady-state PL (at 335 nm). The temporal evolution of the PL further confirms that each surface functional group is responsible for one fluorescence emission peak. Furthermore, the evident dual-emission, centered around 335 and 430 nm, in the time-resolved and steady state PL spectra of C-dots at short-wavelength excitations suggests that these surface states are isolated without effective relaxation between the surface sites [19].

The PL dynamics of C-dots detected around the fluorescence peaks are monitored with excitation wavelengths of 273 and 343 nm, as shown in Fig. S10. All the fluorescence transients are well fitted with double-exponential functions; the best-fit parameters are listed in Table S2. The PL dynamics exhibit two distinct relaxation time scales, fast (0.8–1.7 ns) and slow (4–10 ns) decays, for both of excitation wavelengths. Both of fast and slow components progressively lengthen with increasing emission wavelengths and average lifetimes increase, which is similar with C-dots in previous reports [19,38]. We previously assigned the fast and slow decays to direct excitation-recombination of carriers on the surface states and a relaxation of carriers from carbogenic-core onto the surface states, respectively [37]. The conclusions are also suitable for the PL dynamics demonstrated here that the decays at 273 and 343 nm excitations correspond to carrier dynamics of the surface states created by C=O and C–O groups, respectively. The slow decays show significant different for each excitations (4–6 ns and 9–10 ns for 273 and 343 nm excitations, respectively), while there is similar fast decays with relaxation time around 0.8–1.7 ns for both excitations (Fig. 5b, Table S2). Previous study on surface-related emission in semiconductor quantum dots suggested that the poor overlap of carrier wave functions on surface sites prolong
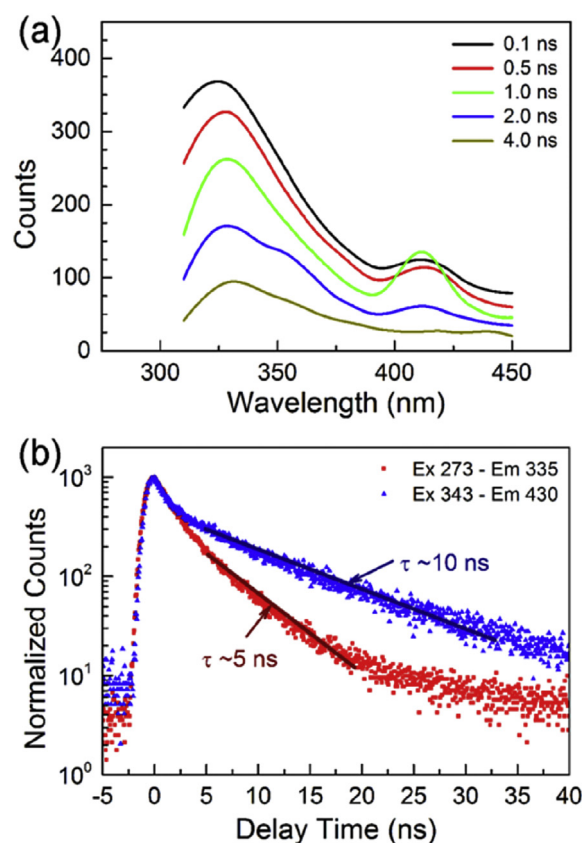

Fig. 5. (a) Time-resolved PL spectra of C-dots after 2 h UV light irradiation at 273 nm excitation. (b) PL dynamics of C-dots after 2 h UV light irradiation at detected wavelengths of 335, 430 nm with 273 and 343 nm excitations, respectively. (A colour version of this figure can be viewed online.)

radiative lifetime [39]. Thus, the deference in slow decays might be attributed to the different overlap degrees of photogenerated electron from carbogenic-core and hole wave functions in these surface functional groups.

4. Conclusions

In summary, a facile method to independent control of the carbogenic-core size and surface chemicals has been developed for PL mechanism study of C-dots. Detailed characterizations proved that the strong fluorescence in C-dots is originated from abundant surface functional groups on its surface, rather than originating from its carbogenic-core. One kind of surface functional group may forms a surface state energy level and becomes an isolated emission center with specific carrier dynamics on the surface site of C-dots. The energy gap of each surface state exhibits carbogenic-core size independent and is characterized by distinct central energies, such as C=O group at 335 nm, and C–O group at 430 nm.

Appendix A. Supplementary data

Supplementary data related to this article can be found at http://dx.doi.org/10.1016/j.carbon.2016.07.019.

References

[1] S.N. Baker, G.A. Baker, Luminescent carbon nanodots: emergent nanolights, Angew. Chem. Int. Ed. 49 (2010) 6726–6744.
[2] K. Hola, Y. Zhang, Y. Wang, E.P. Giannelis, R. Zboril, A.L. Rogach, Carbon dots—emerging light emitters for bioimaging, cancer therapy and optoelectronics, Nano Today 9 (2014) 590–603.
[3] V. Nguyen, L. Yan, J. Si, X. Hou, Femtosecond laser-induced size reduction of carbon nanodots in solution: effect of laser fluence, spot size, and irradiation time, J. Appl. Phys. 117 (2015) 084304.
[4] D. Tan, S. Zhou, B. Xu, P. Chen, Y. Shimotsuma, K. Miura, et al., Simple synthesis of ultra-small nanodiamonds with tunable size and photoluminescence, Carbon 62 (2013) 374–381.
[5] J. Wang, F. Peng, Y. Lu, Y. Zhong, S. Wang, M. Xu, et al., Large-scale green synthesis of fluorescent carbon nanodots and their use in optics applications, Adv. Opt. Mater. 3 (2015) 103–111.
[6] S. Zhu, Q. Meng, L. Wang, J. Zhang, Y. Song, H. Jin, et al., Highly photoluminescent carbon dots for multicolor patterning, sensors, and bioimaging, Angew. Chem. Int. Ed. 52 (2013) 3953–3957.
[7] Z.L. Wu, M.X. Gao, T.T. Wang, X.Y. Wan, L.L. Zheng, C.Z. Huang, A general quantitative pH sensor developed with dicyandiamide N-doped high quantum yield graphene quantum dots, Nanoscale 6 (2014) 3868–3874.
[8] H. Li, X. He, Y. Liu, H. Huang, S. Lian, S.-T. Lee, et al., One-step ultrasonic synthesis of water-soluble carbon nanoparticles with excellent photoluminescent properties, Carbon 49 (2011) 605–609.
[9] L. Tang, R. Ji, X. Cao, J. Lin, H. Jiang, X. Li, et al., Deep ultraviolet photoluminescence of water-soluble self-passivated graphene quantum dots, Acs Nano 6 (2012) 5102–5110.
[10] J. Tang, B. Kong, H. Wu, M. Xu, Y. Wang, Y. Wang, et al., Carbon nanodots featuring efficient FRET for real-time monitoring of drug delivery and two-photon imaging, Adv. Mater. 25 (2013) 6569–6574.
[11] W. Shi, X. Li, H. Ma, A tunable ratiometric pH sensor based on carbon nanodots for the quantitative measurement of the intracellular pH of whole cells, Angew. Chem. Int. Ed. 51 (2012) 6432–6435.
[12] V. Nguyen, L. Yan, J. Si, X. Hou, Femtosecond laser-assisted synthesis of highly photoluminescent carbon nanodots for Fe^{3+} detection with high sensitivity and selectivity, Opt. Mater. Express 6 (2016) 312–320.
[13] W. Kwon, S. Do, J. Lee, S. Hwang, J.K. Kim, S.-W. Rhee, Freestanding luminescent films of nitrogen-rich carbon nanodots toward large-scale phosphor-based white-light-emitting devices, Chem. Mater. 25 (2013) 1893–1899.
[14] X. Zhang, Y. Zhang, Y. Wang, S. Kalytchuk, S.V. Kershaw, Y. Wang, et al., Color-switchable electroluminescence of carbon dot light-emitting diodes, Acs Nano 7 (2013) 11234–11241.
[15] W. Kwon, S. Do, J.H. Kim, M. Seok Jeong, S.W. Rhee, Control of photoluminescence of carbon nanodots via surface functionalization using para-substituted anilines, Sci. Rep. 5 (2015) 12604.
[16] W.F. Zhang, H. Zhu, S.F. Yu, H.Y. Yang, Observation of lasing emission from carbon nanodots in organic solvents, Adv. Mater. 24 (2012) 2263–2267.
[17] S. Qu, X. Liu, X. Guo, M. Chu, L. Zhang, D. Shen, Amplified spontaneous green emission and lasing emission from carbon nanoparticles, Adv. Funct. Mater. 24 (2014) 2689–2695.
[18] V. Strauss, J.T. Margraf, C. Dolle, B. Butz, T.J. Nacken, J. Walter, et al., Carbon nanodots: toward a comprehensive understanding of their photoluminescence, J. Am. Chem. Soc. 136 (2014) 17308–17316.
[19] X. Wen, P. Yu, Y.-R. Toh, X. Hao, J. Tang, Intrinsic and extrinsic fluorescence in carbon nanodots: ultrafast time-resolved fluorescence and carrier dynamics, Adv. Opt. Mater. 1 (2013) 173–178.
[20] P. Yu, X. Wen, Y.-R. Toh, J. Tang, Temperature-dependent fluorescence in carbon dots, J. Phys. Chem. C 116 (2012) 25552–25557.
[21] M.J. Krysmann, A. Kelarakis, P. Dallas, E.P. Giannelis, Formation mechanism of carbogenic nanoparticles with dual photoluminescence emission, J. Am. Chem. Soc. 134 (2012) 747–750.
[22] L. Wang, S.J. Zhu, H.Y. Wang, S.N. Qu, Y.L. Zhang, J.H. Zhang, et al., Common origin of green luminescence in carbon nanodots and graphene quantum dots, Acs Nano 8 (2014) 2541–2547.
[23] S. Ghosh, A.M. Chizhik, N. Karedla, M.O. Dekaliuk, I. Gregor, H. Schuhmann, et al., Photoluminescence of carbon nanodots: dipole emission centers and electron-phonon coupling, Nano Lett. 14 (2014) 5656–5661.
[24] H. Ding, S.-B. Yu, J.-S. Wei, H.-M. Xiong, Full-color light-emitting carbon dots with a surface-state-controlled luminescence mechanism, Acs Nano 10 (2016) 484–491.
[25] K. Jiang, S. Sun, L. Zhang, Y. Lu, A. Wu, C. Cai, et al., Red, green, and blue luminescence by carbon dots: full-color emission tuning and multicolor cellular imaging, Angew. Chem. Int. Ed. 54 (2015) 5360–5363.
[26] L. Bao, C. Liu, Z.L. Zhang, D.W. Pang, Photoluminescence-tunable carbon nanodots: surface-state energy-gap tuning, Adv. Mater. 27 (2015) 1663–1667.
[27] H. Nie, M. Li, Q. Li, S. Liang, Y. Tan, L. Sheng, et al., Carbon dots with continuously tunable full-color emission and their application in ratiometric pH sensing, Chem. Mater. 26 (2014) 3104–3112.
[28] K. Hola, A.B. Bourlinos, O. Kozak, K. Berka, K.M. Siskova, M. Havrdova, et al., Photoluminescence effects of graphitic core size and surface functional groups in carbon dots: COO− induced red-shift emission, Carbon 70 (2014) 279–286.
[29] Z. Gan, X. Wu, Y. Hao, The mechanism of blue photoluminescence from carbon nanodots, CrystEngComm 16 (2014) 4981–4986.
[30] H. Zeng, X.-W. Du, S.C. Singh, S.A. Kulinich, S. Yang, J. He, et al., Nanomaterials via laser ablation/irradiation in liquid: a review, Adv. Funct. Mater. 22 (2012) 1333–1353.
[31] D. Werner, S. Hashimoto, Controlling the pulsed-laser-induced size reduction of Au and Ag nanoparticles via changes in the external pressure, laser intensity, and excitation wavelength, Langmuir 29 (2013) 1295–1302.
[32] C. Carrillo-Carrion, S. Cardenas, B.M. Simonet, M. Valcarcel, Quantum dots luminescence enhancement due to illumination with UV/Vis light, Chem. Commun. (2009) 5214–5226.
[33] Y. Dong, H. Pang, H.B. Yang, C. Guo, J. Shao, Y. Chi, et al., Carbon-based dots co-doped with nitrogen and sulfur for high quantum yield and excitation-independent emission, Angew. Chem. Int. Ed. 52 (2013) 7800–7804.
[34] S. Zhu, J. Zhang, S. Tang, C. Qiao, L. Wang, H. Wang, et al., Surface chemistry routes to modulate the photoluminescence of graphene quantum dots: from fluorescence mechanism to up-conversion bioimaging applications, Adv. Funct. Mater. 22 (2012) 4732–4740.
[35] Z.-Q. Xu, L.-Y. Yang, X.-Y. Fan, J.-C. Jin, J. Mei, W. Peng, et al., Low temperature synthesis of highly stable phosphate functionalized two color carbon nanodots and their application in cell imaging, Carbon 66 (2014) 351–360.
[36] M.K. Barman, B. Jana, S. Bhattacharyya, A. Patra, Photophysical properties of doped carbon dots (N, P, and B) and their influence on electron/hole transfer in carbon dots—nickel (II) phthalocyanine conjugates, J. Phys. Chem. C 118 (2014) 20034–20041.
[37] V. Nguyen, J. Si, L. Yan, X. Hou, Electron—hole recombination dynamics in carbon nanodots, Carbon 95 (2015) 659–663.
[38] L. Bao, Z.L. Zhang, Z.Q. Tian, L. Zhang, C. Liu, Y. Lin, et al., Electrochemical tuning of luminescent carbon nanodots: from preparation to luminescence mechanism, Adv. Mater. 23 (2011) 5801–5806.
[39] X.Y. Wang, L.H. Qu, J.Y. Zhang, X.G. Peng, M. Xiao, Surface-related emission in highly luminescent CdSe quantum dots, Nano Lett. 3 (2003) 1103–1106.